This is a repository copy of *The effect of biomass ashes and potassium salts on MEA degradation for BECCS*.

Article:

The effect of biomass ashes and potassium salts on MEA degradation for BECCS

Diarmaid S. Clery [a,b], Patrick E. Mason [b], Douglas C. Barnes [c], János Szuhánszki [d], Muhammad Akram [d], Jenny M. Jones [b], Mohamed Pourkashanian [d], Christopher M. Rayner [a,c,*]

[a] School of Chemistry, University of Leeds, Leeds, LS2 9JT, UK
[b] School of Chemical and Process Engineering (SCaPE), University of Leeds, Leeds, LS2 9JT, UK
[c] C-Capture Limited, Unit 14, Evans Business Centre, Albion Way, Leeds, LS12 2EP, UK
[d] Energy 2050, Department of Mechanical Engineering, University of Sheffield, Sheffield, S10 2TN, UK

ABSTRACT

This study investigates the comparative impact of inherently different biomass and coal ashes on the laboratory and pilot scale degradation of 30 wt% aqueous monoethanolamine (MEA), relevant to post-combustion CO_2 capture. Thermal and oxidative degradation experiments were carried out at 135 °C and 40 °C respectively with CO_2 loading (0.5 mol_{CO2}/mol_{MEA}), with and without the presence of ash. Nuclear magnetic resonance (NMR) data is provided for the major MEA degradation compounds such as *N*-(2-hydroxyethyl)formamide (HEF) and *N*-(2-hydroxyethyl)imidazole (HEI) along with the characterisation of a new MEA oxidative degradation product, *N*-(2-hydroxyethyl)imidazole-*N*-oxide (HEINO) which had been previously misassigned. Degradation products were quantified using ^{1}H NMR and gas chromatography mass spectrometry (GC–MS) to assess the impact of potassium and various ashes from combustion (olive, white wood and two types of coal ash) on the rates of amine degradation. Woody biomass fly ashes were found to reduce the presence of the oxidative degradation products. Both types of coal fly ash and the olive biomass ash were found to enhance the formation the newly identified degradation product, HEINO. Solvent samples taken from a pilot scale facility support these laboratory findings.

1. Introduction

Bioenergy with carbon capture and storage (BECCS) is heavily relied upon by most climate mitigation scenarios as a technology for large-scale rollout to meet obligations under the Paris Agreement (Anderson and Peters, 2016; IPCC, 2018). CO_2 capture and storage (CCS) has, until recently, primarily been considered as a technology to mitigate the emissions from coal fired power stations, hence research has focused on this use and identified the catalytic impact of coal fly ashes on amine degradation (Chandan et al., 2014; Da Silva et al., 2012). However, using bioenergy with carbon capture and storage (BECCS) provides the important potential for negative carbon emissions whilst generating power (Bui et al., 2018).

Biomass has many different characteristics compared to coal as a solid fuel for power generation; typically higher in moisture content, low in sulphur content and a different mix of inorganic components. Woody biomass pellets are currently the most commonly used biomass fuel for combustion power plants due to their high energy density, however an array of different biomass options exist.

Monoethanolamine (MEA) is the most well understood solvent of the current technologies available for post-combustion capture (PCC), largely due to its well-established use for the removal of CO_2 from natural gas and recent development as a leading technology for post-combustion CO_2 capture on industrial applications. Efforts are being made to create solvents with lower energy requirements, alongside reduced degradation and corrosivity in order to lower the operational costs associated carbon capture (Wheatley et al., 2019), however MEA remains an important benchmark to which other solvent technologies are compared.

The flue gases from both biomass and coal are mostly comprised of N_2, CO_2, O_2, H_2O and NOx along with other minor impurities. Biomass flue gases are typically much lower in SOx content than coal flue gases and coal fly ashes have higher quantities of Fe, Al and Si whereas biomass has higher amounts of K (Finney et al., 2018). However the impacts of biomass fly ashes on amine degradation has not yet been reported in any detail. Biomass power stations are fitted with highly

efficient (>99.9 %) pollutant removal technologies such as electrostatic precipitators (ESP) or fabric filters, however it is still plausible that small quantities of fly ash and flue gas impurities will reach carbon capture facilities. Potassium from biomass is known to volatilise under the high temperatures of combustion (Clery et al., 2018; Jones et al., 2007; Knudsen et al., 2004; Mason et al., 2016) before typically condensing on fine particles or ash deposits. This volatile state may assist K in escaping from emission removal technologies and thus result in higher presence within capture facilities. Quantities of these ashes and volatile species may be small initially but an accumulation effect will occur after prolonged periods of operation. As more degradation products are formed, solvents increase in viscosity and corrosivity, and amine quantities are reduced, resulting in a reduced absorption capacity until the solvent is reclaimed, which has an associated cost and some solvent loss (Dumée et al., 2012). The regeneration of amine solvent is a significant operating cost associated with carbon dioxide removal, therefore understanding the expected impact on the degradation of amine solvents used with biomass combustion is important for the prediction of operational costs at a full-scale BECCS plant.

Previous literature simplifies the complex cyclical heating and cooling of a full-scale CO_2 capture plant into the two types of degradation that would be expected under the conditions of the main capture plant components: Firstly the absorber tower, where the flue gas encounters the solvent and captures the CO_2 – which is represented by oxidative degradation experiments at low temperature and in the presence of oxygen. Second, the stripper (desorber) unit, where the CO_2 rich solvent is heated (120 °C) causing the CO_2 to be released and the solvent to be regenerated – represented by thermal degradation experiments at high temperatures in the absence of oxygen (although some of the results in this paper suggest this is a gross simplification and will need to be reviewed, *vide infra*).

Previous research in this area has identified 2-oxazolidone (OZD), *N*-(2-hydroxyethyl)ethylenediamine (HEEDA) and 1-(2-hydroxyethyl) imidazolidone (HEIA) to be the main degradation products formed under thermal degradation conditions with suggested mechanisms (Da Silva et al., 2012; Davis and Rochelle, 2009; Lepaumier et al., 2009b; Polderman et al., 1955). Many products have been identified from the oxidative degradation of MEA including ammonia, volatile aldehydes, carboxylic acids and major degradation products formed from these smaller compounds such as *N*-(2-hydroxyethyl)imidazole (HEI) and the corresponding *N*-oxide (HEINO, *this work, vide infra*), and *N*-(2-hydroxyethyl)formamide (HEF) (Fig. 1) (Da Silva et al., 2012; Goff and Rochelle, 2006; Rooney et al., 1998; Sexton and Rochelle, 2006). *N, N'*-bis(2-hydroxyethyl)oxalamide (BHEOX), 4-(2-hydroxyethyl)piperazin-2-one (HEPO) and *N*-(2-hydroxyethyl)-glycine (HEGly) were not examined in this study due to the small quantities found in laboratory

oxidative degradations in previous literature (Da Silva et al., 2012; Lepaumier et al., 2009a). Previous research found the oxidation of MEA to be catalysed by redox active metals such as Fe and Cu when dissolved in the solvent solution which can leach from stainless steels used for the construction of PCC equipment (Goff, 2005). Oxidative degradation is the dominant form of degradation in pilot-scale carbon capture facilities (Da Silva et al., 2012; Strazisar et al., 2003), with thermal degradation products not being detected in some cases (Léonard et al., 2015). An early pilot-scale study found high levels of potassium, sodium, calcium and iron cations in the solvent used, along with high chloride, sulphate, fluoride and nitrate anion concentrations believed to originate from the coal fuel used in the study (Strazisar et al., 2003).

The current work builds on previous work examining the degradation of MEA in the presence of biomass ashes and potassium salts, under laboratory conditions, and also at pilot-scale through the use of a 250 kW combustion furnace fitted with a pilot-scale CO_2 capture facility. Laboratory experiments to examine the thermal degradation of MEA were carried out using closed-batch experiments at 135 °C in the presence of full CO_2 loadings (0.5 mol_{CO2}/mol_{MEA}). Degradation experiments in the absence of CO_2 loading were excluded from this work due to the lack of degradation seen with such conditions (Da Silva et al., 2012). Laboratory experiments to investigate oxidative degradation of MEA used an open-batch system at 40 °C with compressed air bubbled through solvents at 0.15 L/min with full CO_2 loading (similar to Da Silva et al., 2012). The impacts of adding biomass ashes, coal ashes and KCl to laboratory experiments was investigated. The laboratory experiments were compared with CO_2 loaded MEA samples obtained from a 250 kW combustion furnace and a pilot-scale CO_2 capture facility, run separately on biomass and coal flue gases. All samples (from laboratory and pilot plant experiments) were analysed by the same techniques: proton nuclear magnetic resonance (^{1}H NMR) and gas chromatography – mass spectrometry (GC – MS) for product formation, and inductively coupled plasma optical emission spectrometry (ICP-OES) for leached metals quantification.

2. Experimental methods

2.1. Chemicals and ashes

MEA (ethanolamine) and KCl (99 % purity) were purchased from Alfa Aesar. mCPBA, OZD, HEEDA, HEIA, HEI, HEF, HEA and BHEOX were all purchased from Sigma Aldrich. These chemicals were used for product identification and equipment calibration.

The Pilot-scale Advanced Capture Technology (PACT) facilities in Sheffield, UK provided two fly ash samples used by this study: a coal ash and a wood ash. Five ashes were used in total by this study: PACT coal
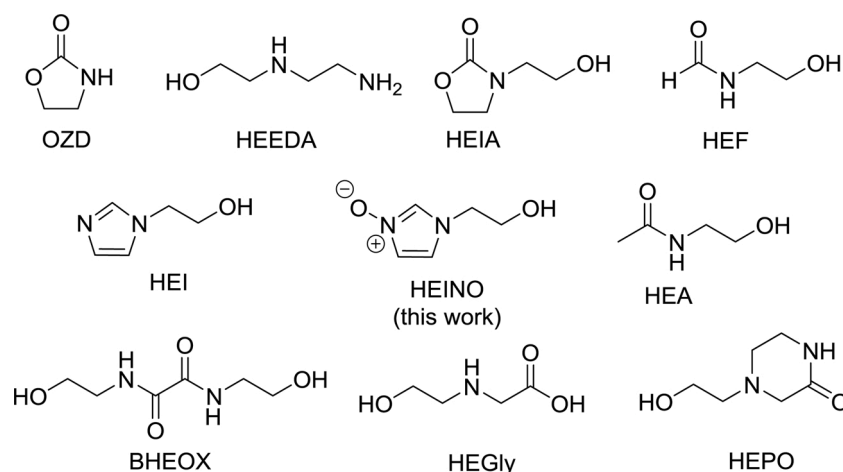

Fig. 1. Major thermal, oxidative and pilot plant degradation products of monoethanolamine (MEA).

ash, PACT wood ash, coal ash #1, olive ash and white wood ash. Coal ash #1 was provided by a coal fired UK power station. The olive ash and white wood ash were prepared from the combustion of milled olive-processing residues and graded wood pellets for industrial use using a Carbolite AAF 1100 furnace in accordance with the European Standard methods for the determination of ash (EN 18,122). All ash samples were characterised by SOCOTEC UK Limited.

2.2. Laboratory-scale thermal MEA degradations

Thermal degradation experiments were carried out using stainless steel batch reactors stored under heated conditions (135 °C) as the most established method for examining the effects of thermal degradation within the laboratory (Davis and Rochelle, 2009; Léonard et al., 2015; Lepaumier et al., 2011). To investigate the impact of biomass ash and potassium chloride on the thermal degradation of MEA in the presence of CO_2, a batch of 30 wt% MEA solution (150 mL, prepared using deionised water), was sparged with CO_2 at a rate of 0.3 L/min for 120 min to obtain a loading of 0.5 mol of CO_2 per mole of amine, which was confirmed with NMR spectroscopy. Small samples (20 mL) of the loaded solution were poured into a 2-inch diameter 304 stainless steel cylinders purchased from StillDragon Europe, which were then sealed using an end cap, tri-clamp and Teflon gasket before being kept in a Memmert oven (model 600) at 135 °C for 6 weeks.

The compositional data for the white wood ash and coal ash #1 used in the thermal MEA degradation experiments are provided in Table 1. The white wood ash was prepared using a Carbolite AAF 1100 furnace at 550 °C in accordance with the European Standard methods for the determination of ash (EN 18122). The coal ash #1 is a fly ash from a coal fired UK power station. The quantities of ash added to each degradation were in line with previous literature (Da Silva et al., 2012) at 3.4 g of ash per kilogram of MEA solution, equating to 0.068 g of ash in the MEA samples (20 mL) used in these thermal degradation experiments.

To examine the effect of KCl on thermal MEA degradation 30 mM KCl (99 %) was added to the amine solvent, equating to 45 mg in the small samples (20 mL) used in these experiments as an exaggeration of the highest quantities of KCl that are likely to be deposited in a capture solvent.

2.3. Laboratory-scale oxidative MEA degradations

To investigate the impact of biomass ash and potassium salts on the oxidative degradation of MEA, an apparatus set-up similar to previous MEA oxidation experiments was used (Da Silva et al., 2012): An MEA solution (30 wt% prepared using deionised water, 250 mL) was placed in a 500 mL round bottom flask fitted with air and CO_2 sparger, and warmed to 40 °C, as illustrated in Fig. 2. The solution was initially loaded fully (α =0.5 mol of CO_2 per mole of amine) by sparging 0.3 L/min of CO_2 through the solvent for 2 h. This was followed by a sparging of compressed air at 0.15 L/min for 21 days, with periodic sparging with CO_2 (0.3 L/min for 30 min every 3 days) to regenerate or maintain a high loading level – essential to the oxidative degradation process. Small aliquots (5 mL) were taken every 3 days in order to track

the degradation.

The compressed air was first sparged through water to saturate the air and minimise any moisture losses in the solvent round bottom flask which would affect the measured MEA concentrations in solution. Volumes of solvent were measured before and after experiments, however no significant water losses were seen throughout the degradation experiments.

The compositional data for the four ashes used in the oxidative degradation experiments (PACT wood ash, PACT coal ash, coal ash #1 and olive ash) are provided in Table 2. Two of these ashes were collected from the candle filter at the PACT facilities during the combustion of woody biomass, PACT wood ash, and a coal from the El Cerrejon region, PACT coal ash.

The pilot combustion facility holds a down-fired pulverised fuel furnace operating with interchangeable burners and feeding systems for the firing of biomass and coal solid fuels (Szuhánszki, 2014). Natural gas was used to preheat the furnace with temperatures of 1350 °C at the top of the furnace and approximately 1200 °C just above the heavy fly ash collection water tray. The facilities are fitted with particulate removal equipment similar to that used by a full scale biomass combustion plant - a cyclone was custom built for the facility while the candle filter is a Glosfume ceramic biomass filter unit. Fly ash samples from the candle filter were collected from a large ash collection tray at the bottom of filter at the end of each day, with an hour of firing provided to reach steady state conditions. The ashes were collected from the candle filter apparatus to obtain fine ash samples after firing from the 250 kW air combustion furnace, making the ash composition most similar to those that would be encountered by carbon capture facilities. Coal ash #1 was provided by a coal fired UK power station. The olive ash was prepared by combusting milled olive-processing residues using a Carbolite AAF 1100 furnace at 550 °C in accordance with the European Standard methods for the determination of ash (EN 18122). The quantities of ash added to each degradation are in line with previous literature at 3.4 g of ash per kilogram of MEA solution, equating to 0.85 g ash in the MEA samples (250 mL) used in these experiments.

To examine the effect of KCl on oxidative MEA degradation 23 mM KCl (99 %) was added to the amine solvent, equating to 0.43 g in the MEA samples (250 mL) used in these experiments as an exaggeration of the highest quantities of KCl that are likely to deposit in a capture solvent.

2.4. Pilot-scale MEA degradations

Samples of 30 wt% MEA were obtained from the Pilot-scale Advanced Capture Technology (PACT) facilities in Sheffield, UK. Solvent samples were rich in CO_2 and were taken from the bottom of the absorber tank, so are considered to be loaded, and had been exposed to oxygen but without subsequent thermal treatment in the stripper. The solvent had been used to capture carbon dioxide from the 250 kW pulverised fuel air combustion furnace burning either biomass or coal. These were the same combustion trials from which the PACT wood ash and PACT coal ash samples were obtained for oxidative laboratory degradations described in the previous section. In both cases the solvent was unused prior to the 3 day test campaign. The white wood pellets used are typical of the biomass currently used for biomass power generation in the UK. The biomass used is low in ash and fixed carbon content compared to the coal, but high in volatiles (Finney et al., 2018). The coal has a higher carbon content than biomass and higher in Al, Si and Fe content – all of which are typical for coal. Fe is of particular importance due to its known catalysis of oxidative degradation of amine solvents along with Cu (Sexton and Rochelle, 2009). In contrast, the biomass ash contains higher K and Mn contents than the coal ash – high Mn is also important due to its known activity as an oxidation catalyst.

The pilot combustion facility holds a down-fired pulverised fuel furnace capable of operating in air-fired combustion conditions for biomass and coal (Szuhánszki, 2014). The combustion rig was operated

Table 1
Ash composition data for ashes used in thermal degradations of MEA.

Content[*]	White wood ash	Coal ash #1
Al_2O_3	2.5	20.8
Fe_2O_3	2.1	9.3
CaO	29.3	2.9
MgO	5.9	1.9
Na_2O	2.2	2.3
K_2O	10.0	1.7
Mn_3O_4	2.1	<0.1
SiO_2	16.6	58.2

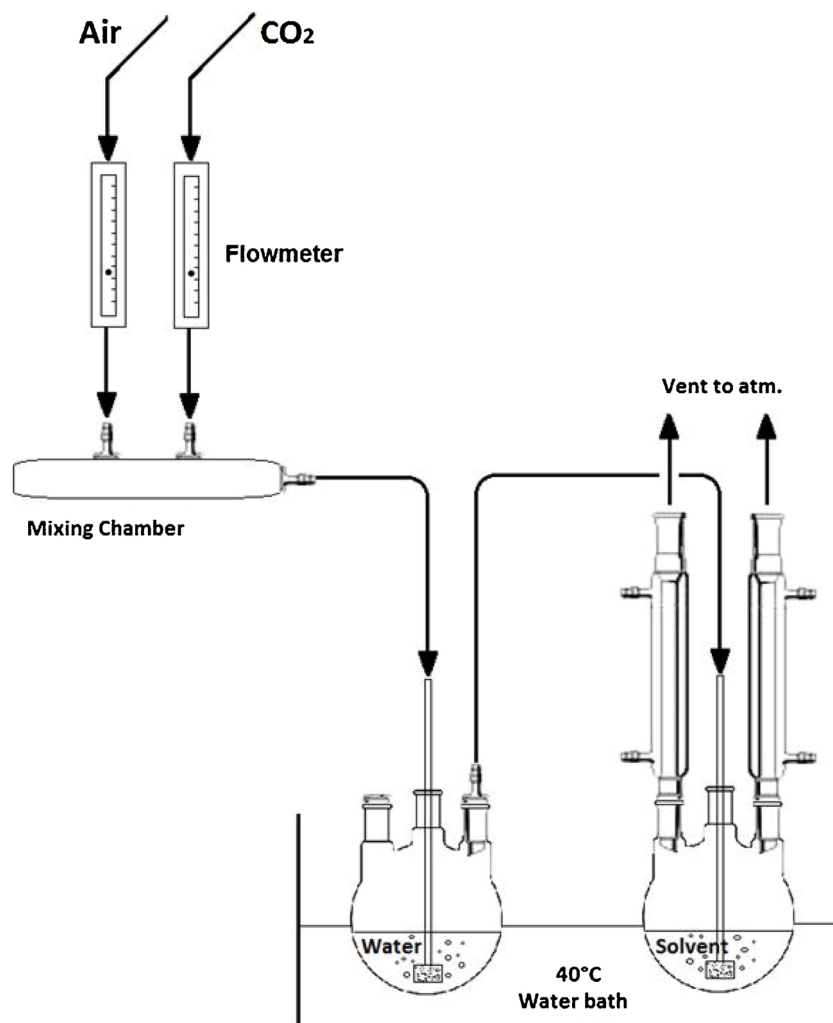[*] All contents reported on a 'percentage in ash' basis.

Fig. 2. Open-batch oxidative degradation set-up.

Table 2
Ash composition data for ashes used in oxidative degradations of MEA.

Content[*]	Olive ash	PACT wood ash	PACT coal ash	Coal ash #1
Al_2O_3	1.2	4.1	19.9	20.8
Fe_2O_3	0.9	4.7	14.3	9.3
CaO	10.3	18.3	19.3	2.9
MgO	3.0	3.8	3.4	1.9
Na_2O	0.6	3.9	4.2	2.3
K_2O	34.8	21.0	1.7	1.7
Mn_3O_4	<0.1	1.9	0.3	<0.1
SiO_2	11.2	7.6	29.6	58.2

[*] All contents reported on a 'percentage in ash' basis.

and monitored by Dr. János Szuhánszki of the University of Sheffield through a local Human-Machine Interface (HMI). The flue gases from the furnace of each trial encounter particle removal technologies, a cyclone and candle filter, the arrangement of these has been provided in previous literature (Finney et al., 2018). After the particulate removal technologies, a flue gas desulphurisation (FGD) system using sodium hydroxide was used for the removal of SO_2 for coal flue gases of two days out of the three day (30 h) trial, as it is a high sulphur fuel. For the biomass trial, the FGD unit was operated as a direct contact cooler (DCC) unit by using water to cool the flue gas as biomass is a lower sulphur content fuel (Finney et al., 2018). A fan is used after the FGD to pressurise the flue gas through the CO_2 absorber where the gas contacts the 30 wt% MEA solvent and CO_2 reacts with the counter flowing solvent

and is thus removed from the flue gas. The FGD and pilot post combustion capture plant was monitored by Dr. Muhammad Akram of the University of Sheffield, who operated the plant during both trials and provided rich MEA samples from the bottom of the absorber tank. Details on the pilot-scale carbon capture plant have been reported previously (Akram et al., 2016).

2.5. Analyses

Proton nuclear magnetic resonance (^{1}H NMR) was employed as the preferred method of quantitative analysis for CO_2 loadings and tracking of the major degradation product formation. Gas chromatography-mass spectrometry (GC–MS) was used to validate these findings and compare degradation rates between the cases with and without ashes or potassium chloride. Inductively coupled plasma optical emission spectrometry (ICP-OES) was used to quantify metals present in the solvent solutions.

2.5.1. Nuclear magnetic resonance (NMR)

In 2014 Perinu et al. published a review of NMR spectroscopy applied to amine capture systems which highlighted the reliability of ^{1}H and ^{13}C NMR for fast and reliable method for the quantitative analyse of many common species associated with the absorption of CO_2 by MEA solutions. This included the identification and quantification of MEA, carbamate, and oxidative degradation products (Ciftja et al., 2012; Wheatley et al., 2019). Therefore the current work used ^{1}H and ^{13}C NMR

analysis to monitor the CO_2 loadings of samples throughout the duration of experiments and the formation of major degradation products (OZD, HEEDA, HEIA, HEI and HEF).

Fig. 3 illustrates how the chemical shifts of MEA in water arise at 3.57 ppm and 2.71 ppm. Increasing quantities of CO_2 added to the 30 wt % MEA sample, the MEA peaks are seen to move further downfield and the carbamate peaks are seen to increase as a triplet at 3.58 ppm and multiplet at 3.15 ppm. MEA signals move further downfield as it reacts with CO_2 to form the carbamate and the protonated amine base, however the rate of proton exchange between the free base and the protonated base is considerably faster than the NMR timeframe, hence the peaks seen are a combination of the two forms (Wheatley, 2017). As more CO_2 is absorbed by the solvent, more and more protonated MEA is formed, thus explaining the movement of the peaks seen for MEA. The chemical shifts for the protons and carbons associated with MEA, carbamate and the degradation products are provided in Table 3.

For both thermal and oxidative degradations, ^{1}H NMR spectroscopy was used to identify and quantify the products formed from aqueous MEA. A small aliquot of the solvent (0.5 mL) was added to an NMR tube along with D_2O (75 μL) to provide a lock frequency. Approximately 100 mg of each purchased degradation product was weighed into D_2O (0.5 mL) to obtain a NMR spectra for each pure product as a reference. The NMR data for the pure products could then be used to identity the spectroscopic peaks from the degraded MEA samples in D_2O. Samples of the degraded solvent were also spiked with the purchased or independently synthesised degradation products to confirm these chemical shifts under sample conditions, where factors such as pH and concentration can influence shift measurements.

NMR spectra were obtained using Bruker Avance III HD-400 spectrometer operating at 400 MHz for ^{1}H and 100 MHz for [13]C. D_2O was employed as the most commonly used compound (Perinu et al., 2014) to provide a deuterium lock for the spectrometer and 4,4-dimethyl-4-silapentane-1-sulfonic acid (DSS) was used as a reference peak, with $\delta = 0$. A solution of 13 mg of DSS was prepared in D_2O (10 mL) for the addition of 75 μL to each NMR sample. Chemical shifts were recorded downfield from this DSS peak at 0 ppm, with product peaks integrated with respect to the known quantity of DSS, in order to calculate the quantities of each degradation product. Proton and carbon assignments in this work are based on an appropriate combination of correlation spectroscopy (COSY), heteronuclear multiple-bond correlation spectroscopy (HMBC) and heteronuclear multiple-quantum correlation

spectroscopy (HMQC) as forms of two-dimensional nuclear magnetic resonance (2D NMR) analysis methods that can be used to identify which proton shifts correlate with neighbouring proton or carbon shifts. NMR data is reported using the following abbreviations; s = singlet, d = doublet, t = triplet.

Fig. 4 shows a stacked NMR spectra for the oxidative degradation experiments whereby signals for MEA (Fig. 3) are enlarged off scale, so the lower level impurity signals are now clearly visible. From the stacked plot it can be observed that oxidative product peaks are seen to grow in the aromatic region (6.5−9 ppm) of the NMR spectra (and others) over the experimental period. These peaks were assigned to the associated degradation product by comparison with NMR spectra of the pure products and spiking of degraded MEA samples.

2.5.2. Gas chromatography-mass spectrometry (GC–MS)

GC–MS was used for analysis of volatile amine degradation products. The degraded solvent (1 mL) was placed in a 2 mL borosilicate glass vial before being covered with aluminium crimp seals and loaded in to the GC–MS autosampler. Analyses were complete using a Perkin Elmer Clarus 580 gas chromatograph equipped with an autosampler and Perkin Elmer Clarus 560 mass spectrometer (inert XL EI/CI MSD with triple axis detector). A Rtx-35 Amine Column (30 m x0.32 mm x1.00 μm) with helium carrier gas was used for separation of the degradation products with an initial oven temperature of 100 °C held for 10 min, followed by a ramp rate of 5 °C/min to 250 °C where it was held for 10 min, (InjAauto =250 °C, Split = 5:1, Solvent Delay =2.50 min, Transfer Temp =250 °C - Source Temp =180 °C, Scan: 10–300 Da). Calibration standards were made for each of the degradation products to enable peak identification and calibration curves of known degradation products. The times for the associated elution of HEEDA, HEF, OZD, HEI and HEIA were 12.3 min, 17.3 min, 21.2 min, 24.6 min and 34.4 min respectively, which were confirmed with doped sample runs.

2.5.3. Inductively coupled plasma optical emission spectrometry (ICP-OES)

The samples of 30 wt% MEA that were subjected to the degradation conditions described previous were analysed by inductively coupled plasma - optical emission spectrometry (ICP-OES) to measure the quantities of elements that had leached into the MEA solution. This enables analysis of the key elements that could affect the degradation. A Thermo Fisher iCAP 7400 Radial ICP-OES was used to measure concentrations of Al, Mg, Ca, Mn, Pb, Ni, Cu, Cr, K, Na, Fe and Si as the key
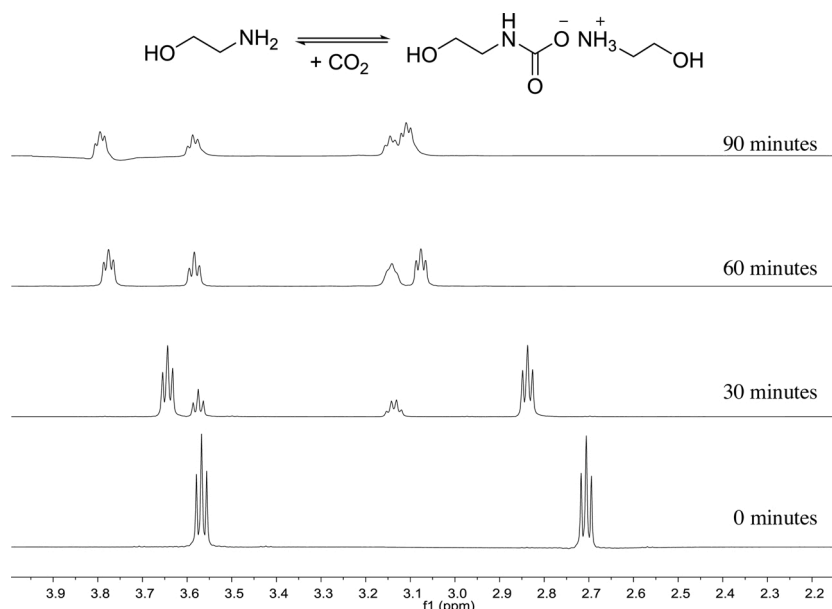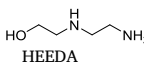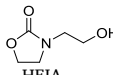

Fig. 3. ^{1}H NMR stacked spectra for the carboxylation of 30 wt% MEA.

Table 3
Typical NMR chemical shifts for the carboxylation of MEA and degradation products.

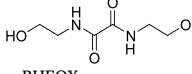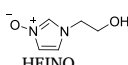| Compound	^{1}H NMR Data (D$_2$O)	^{13}C NMR Data
MEA (HO–CH$_2$CH$_2$–NH$_2$)	3.57 (t, 2H, $^3J_{HH}$ = 5.5 Hz, OCH$_2$)	57.7 (HOCH$_2$)
	2.71 (t, 2H, $^3J_{HH}$ = 5.5 Hz, NCH$_2$)	41.2 (NCH$_2$)
carbamate	3.58 (t, 2H, $^3J_{HH}$ = 5.5 Hz, OCH$_2$)	164.3 (C=O)
	3.15 (dt, 2H, $^3J_{HH}$ = 5.5, 5.0 Hz, NCH$_2$)	61.1 (HOCH$_2$)
		43.1 (NCH$_2$)
	n/a	160.6
Thermal degradation products		
OZD	4.49 (t, 1H, $^3J_{HH}$ = 8.5 Hz, O–CH$_2$)	162.7 (C=O)
		66.1 (OCH$_2$)
	3.65 (t, 1H, $^3J_{HH}$ = 8.5 Hz, N–CH$_2$)	40.5 (NCH$_2$)
HEEDA	3.65 (t, 2H, $^3J_{HH}$ = 5.5 Hz, HOCH$_2$)	60.4 (HOCH$_2$)
	2.68-2.72 (m, 4H, HNCH$_2$)	50.6 (HNCH$_2$)
		49.9 (HNCH$_2$)
	2.63 (t, 2H, $^3J_{HH}$ = 4.8 Hz, H$_2$NCH$_2$)	40.0 (H$_2$NCH$_2$)
HEIA	3.70 (t, 2H, $^3J_{HH}$ = 5.5 Hz, HOCH$_2$)	164.9 (C=O)
	3.56 (t, 2H, $^3J_{HH}$ = 8.0 Hz, OCH$_2$)	58.9 (HOCH)
	3.43 (t, 2H, $^3J_{HH}$ = 8.0 Hz, NCH$_2$)	45.4 (OCH$_2$)
	3.27 (t, 2H, $^3J_{HH}$ = 5.5 Hz, NCH$_2$)	45.2 (NCH$_2$)
		38.1 (NCH$_2$)
Oxidative degradation products		
HEI	7.69 (s, 1H, CH)	138.3 (C=N)
	7.19 (d, 2H, $^3J_{HH}$ = 0.8 Hz, CH)	127.7 (C=C)
	7.05 (d, 2H, $^3J_{HH}$ = 0.8 Hz, CH)	120.2 (C=C)
	4.12 (t, 2H, $^3J_{HH}$ = 5.6 Hz, OCH$_2$)	60.8 (OCH$_2$)
	3.85 (t, 2H, $^3J_{HH}$ = 5.6 Hz, NCH$_2$)	48.9 (NCH$_2$)
HEF	8.09 (s, 1H, CHO)	164.5 (C=O)
	3.67 (t, 2H, $^3J_{HH}$ = 5.6 Hz, OCH$_2$)	59.8 (OCH$_2$)
	3.37 (t, 2H, $^3J_{HH}$ = 5.2 Hz, NCH$_2$)	40.1 (NCH$_2$)
HEA	8.00 (s, 1H, NH)	174.5 (C=O)
	3.65 (t, 2H, $^3J_{HH}$ = 5.6 Hz, OCH$_2$)	59.9 (OCH$_2$)
	3.32 (t, 2H, $^3J_{HH}$ = 5.6 Hz, NCH$_2$)	41.5 (NCH$_2$)
	2.00 (s, 1H, CCH$_3$)	21.8 (CCH$_3$)
BHEOX	3.72 (t, 2H, $^3J_{HH}$ = 5.6 Hz, OCH$_2$)	161.1 (C=O)
		59.7 (OCH$_2$)
	3.45 (t, 2H, $^3J_{HH}$ = 5.6 Hz, NCH$_2$)	41.6 (NCH$_2$)
HEINO (this work)	8.25 (app t, 1H, $^3J_{HH}$ = 2.0 Hz, N$^+$CHN)	127.8 (N$^+$CHN)
	7.20 (app t, 1H, $^3J_{HH}$ = 2.0 Hz, N$^+$CH)	120.3 (N$^+$CH)
	7.16 (app t, 1H, $^3J_{HH}$ = 2.0 Hz, NCH)	118.9 (NCH)
	4.15 (t, 2H, $^3J_{HH}$ = 5.2 Hz, OCH$_2$)	60.2 (OCH$_2$)
	3.85 (t, 2H, $^3J_{HH}$ = 5.2 Hz, NCH$_2$)	51.2 (NCH$_2$)

constituents of biomass and coal ashes. The equipment was operated by Stephen Reid from the School of Earth and Environment at the University of Leeds.

3. Results

3.1. Laboratory-scale thermal degradations

The main thermal degradation compounds reported in previous work were also detected in this study: OZD, HEEDA and HEIA.

Fig. 5 shows the extent of degradation observed for the thermal degradation experiments of 30 wt% MEA (0.5 mol$_{CO2}$/mol$_{MEA}$) at 135 °C after 6 weeks. No significant impact was seen from the addition of potassium chloride, white wood ash or coal ash to the formation of OZD, HEEDA and HEIA. The results show slightly higher levels of HEEDA and HEIA for all cases when compared to the base case of 30 wt% MEA alone however no significant differences are seen in order to suggest the degradation is accelerated or retarded by the ashes or KCl.

Quantification of GC–MS experiments were based on the calibration

of the equipment with known percentages of each degradation product, whereas NMR quantities were calculated by integrating the product chemical shifts compared to the known quantities of DSS in each NMR sample. From this is can be seen that approximately 14 % of HEIA is present in the solvent which equates to nearly half of the original 30 wt % MEA. This finding is concurrent with previous research with expected MEA losses of ~60 % after 5 weeks under such conditions (Da Silva et al., 2012). Importantly, as HEIA is not basic, this renders it inactive as a capture agent, and so accumulation of this degradation product significantly reduces the efficiency of the capture solvent.

The product quantities from NMR were calculated based on integrated product peaks relative to the known quantity of DSS in the sample, thus enabling the absolute amounts of each product to be calculated. Respective masses of each product in the sample were then calculated. These were validated with measurements from GC–MS which was calibrated with known weight percentages of each degradation product in MEA solution (30 wt%). Some slight differences are seen between the analysis techniques for OZD and HEIA – likely due to slight variations in the methodology associated with gas chromatography, whilst the significant difference in quantities of HEEDA are detected between the two analysis techniques. NMR spectra were observed to consistently measure quantities of the degradation products across the cases.

3.2. Laboratory-scale oxidative degradations

The first stage of oxidative MEA degradation involves the oxidation and fragmentation of amines to carboxylic acids, such as formic, acetic, glycolic, and oxalic acid, or volatile species, such as formaldehyde, acetaldehyde or ammonia. Formaldehyde, acetaldehyde and ammonia could not be directly measured due to their reactivity and low concentrations, while the proton chemical shifts associated with formic, acetic and glycolic acids were monitored for the small quantities present in solution.

The main oxidative degradation compounds reported in previous work were also detected in this study: OZD, formic acid, HEF and HEI (Da Silva et al., 2012). One of the key studies previously using ^{1}H NMR analysis for the detailed identification of MEA degradation products (Ciftja et al., 2012) found peaks associated with the oxidative degradation of MEA to be isolated in the 6.5−9 ppm region of NMR spectra, nearly identical to that seen in Fig. 4. This literature study assigned the chemical shifts of the oxidative degradation products in this region to HEI and HEF. However these chemical shifts appear to have been incorrectly assigned in the existing literature. Ciftja et al. assigned the aromatic peaks for HEI as 7.22 ppm, 7.24 ppm and 8.31 ppm, whereas shifts obtained for pure HEI and spiked MEA samples in this work showed shifts at 7.05 ppm, 7.19 ppm and 7.69 ppm. HEF is also incorrectly assigned as 8.48 ppm in the literature, whereas this study confirms a peak at 8.09 ppm. Quantities of HEI and HEF measured by this work are presented in Fig. 6.

Further 2D NMR methods were used to confirm that ^{1}H and ^{13}C peaks corresponded to an unknown degradation product. The corrected ^{1}H and ^{13}C data for HEI are provided in Table 3. The chemical shifts for the unknown compound correspond closely with those found for HEI and thus suggest that the unknown compound is likely an imidazole. 2D NMR revealed ^{13}C NMR shifts associated with the unknown at 119.6 ppm, 120.9 ppm and 128.3 ppm – again characteristic of aromatic compound similar to HEI. Through purification of the compound and careful consideration of the possible heteroaromatics described in (Clery, 2019) it was suspected that the unidentified compound was an oxidation product of HEI as an imidazole with an attached ethanol and oxygen to make an *N*-oxide with M + 1 of 129.

3.2.1. Synthesis of N-(2-hydroxyethyl)imidazole-N-oxide (HEINO)

In order to confirm the correct assignment of the suspected degradation compound the desired *N*-oxide was synthesised. The similarity of
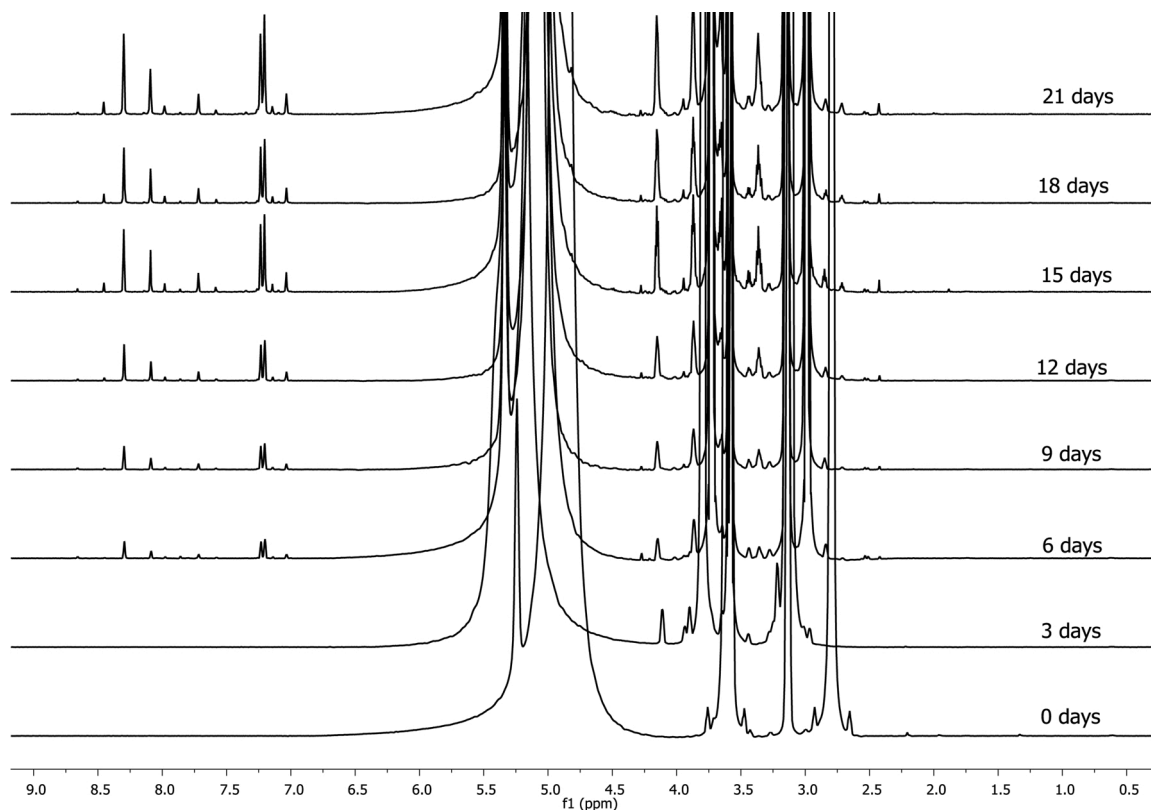
Fig. 4. Example ^{1}H stacked spectra following the oxidative degradation of MEA over 21 days.

the suspected compound to HEI made a logical starting material for further reaction. Aromatic nitrogen heterocycles are well-known to undergo oxidation to the corresponding *N*-oxides with a variety of oxidising agents, although we were unable to find any specific examples of HEI oxidation.

The successful synthesis of *N*-(2-hydroxyethyl)imidazole-*N*-oxide (Scheme 1), abbreviated as HEINO, was carried out by oxidation of *N*-(2-hydroxyethyl)imidazole using meta-chloroperoxybenzoic acid (mCPBA) as follows:

N-(2-Hydroxyethyl)imidazole-*N*-Oxide.

To a stirred solution of *N*-(2-hydroxyethyl)imidazole (5.0 g, 44 mmol) in CH_2Cl_2 (50 mL), a solution of mCPBA (75 %, 23 g, 133 mmol) in CH_2Cl_2 (100 mL) was added dropwise at 0 °C. The reaction mixture was stirred at room temperature for 3 h and monitored by TLC (CH_2Cl_2/MeOH, 80:20). Once complete the reaction was filtered and the solvent removed under reduced pressure. Chromatography on silica eluting with CH_2Cl_2/MeOH (80:20) afforded the title compound as a colourless oil (1.59 g, 12.0 mmol, 28 %). R_f (CH_2Cl_2/MeOH, 80:20) = 0.10. ^{1}H NMR δ(500 MHz; D_2O); 3.85 (2H, t, J 5.2, OCH_2), 4.15 (2H, t, J 5.2, NCH_2), 7.16 (1H, t, J 2.0, NCH), 7.20 (1H, t, J 2.0, N^+CH), 8.25 (1H, t, J 2.0, N^+CHN). DEPTQ ^{13}C NMR δ(125 MHz; D_2O); 51.2 (NCH_2), 60.2 (OCH_2), 118.9 (NCH), 120.3 (N^+CH), 127.8 (N^+CHN). HRMS $C_5H_8N_2O_2$ requires 128.0665; found 128.0656.

Infrared spectroscopy found a peak at 1307 cm^{-1}, matching that previous measured for an *N*-oxide imidazole (Murray, 2016). The HEINO product was found to precisely match the ^{1}H and ^{13}C NMR data of the unknown degradation compound.

3.2.2. Impacts of potassium chloride, biomass ash and coal ash on the oxidative degradation product formation with ^{1}H NMR spectroscopy

Following the identification of the unknown degradation product, the quantities of these oxidative degradation products were plotted over the period of the laboratory experiment. This enabled a comparison of

the quantities of key secondary oxidative degradation products (HEI, HEINO and HEF) in the presence of various ashes – with particular interest in the different rates of degradation that were observed in the presence of ashes from biomass combustion rather than coal.

Fig. 6a) demonstrates the influence that a particular fuel combustion ash can have on the formation of HEI during oxidative degradation. The 'PACT coal ash' is seen to result in a significant increase in the formation of HEI over the 3 week period, with approximately three times greater than the quantities of HEI observed for all other cases including a 'coal ash #1′ sourced form a UK power station. The addition of olive ash and KCl do not appear to have an effect on the formation of HEI whilst the 'PACT wood ash' appears to show slightly lower levels of HEI than the other cases.

Interestingly Fig. 6b) illustrates that both types of coal ash appear to significantly promote the formation of the newly identified HEINO (with chemical shifts at 7.22 and 7.24 ppm). Olive ash also appears to catalyse the formation of this product whilst relatively small quantities of the HEINO are seen for MEA alone, with KCl or 'PACT wood ash'. For HEINO: Olive ash > Coal ash #1 > PACT coal ash > PACT wood ash, whereas for HEF (Fig. 6c), the only noticeable difference between the cases is slightly lower quantities of HEF for the oxidative degradation of MEA in the presence of 'PACT wood ash'.

The formation of HEINO is particularly noteworthy as it is an *N*-oxide, related derivatives of which are known to be capable of oxidising a range of organic substrates, especially in the presence of metal catalysts (Fuentes and Clarke, 2008; He et al., 2012; Niu et al., 2019). Importantly they would also be retained in solution throughout the capture process, until reduced back to HEI, and so act as an oxygen shuttle between the absorber and the stripper. Although oxidative degradation is usually considered to occur mainly in the absorber section of the capture process (where oxygen is present), the formation of HEINO represents a mechanism where oxidation can take place under the more extreme conditions of the stripper or reclaimer, mainly due to the higher temperatures. The reversible nature of HEI oxidation, means
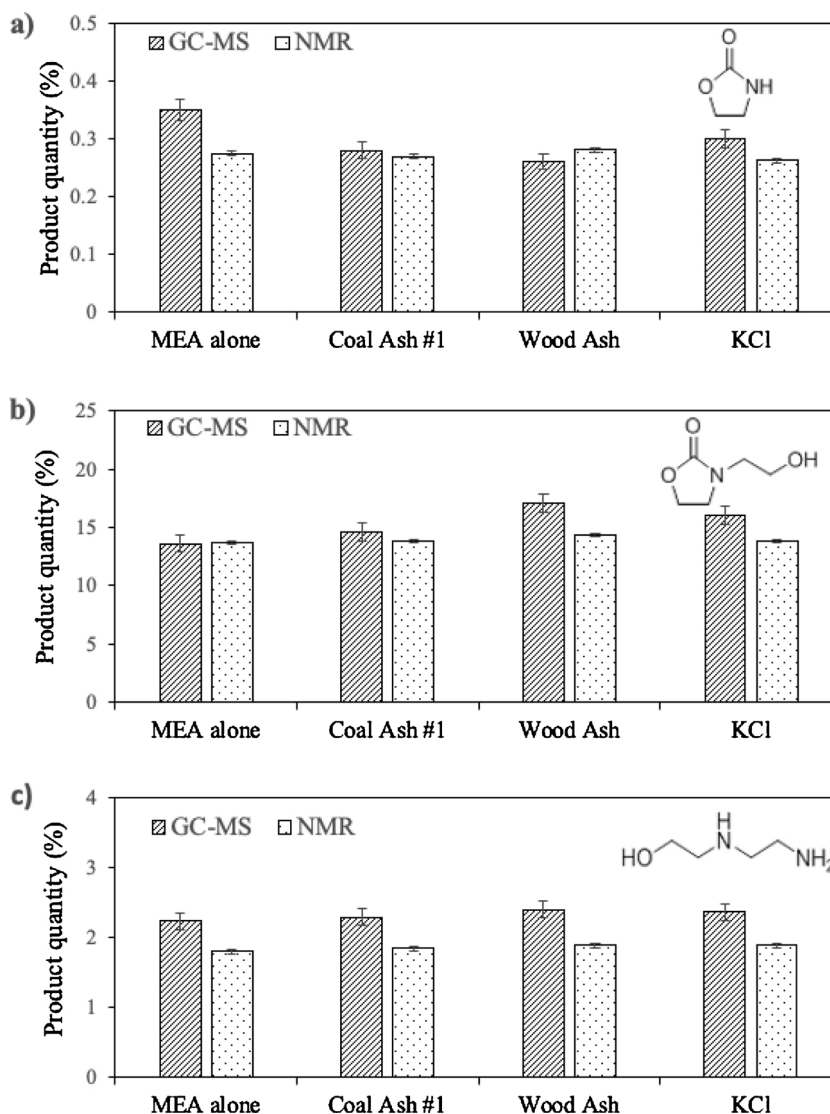
Fig. 5. Product formation of a) OZD b) HEIA and c) HEEDA in the thermal degradation of MEA alone, MEA with coal ash 2, PACT wood ash and KCl.

that as HEI levels build up, potential oxidation is more likely. Depending on sampling of the solvent, only HEI may be present (e.g. in lean going into absorber), or HEINO may be observed (e.g. in loaded solvent coming out of absorber). More detail is required to confirm this and studies are currently underway. In any case, the HEI-HEINO cycle provides a mechanism for oxidation to occur in hotter parts of the process away from the absorber, particularly with partially aged solvent where HEI has had time to build up.

Gas chromatography mass spectrometry (GC–MS) was used as an additional method of analysing degradation product formation. Fig. 7a) illustrates an important difference in the quantities of HEI measured by the two measurement techniques. NMR detected fairly equal amounts of HEI in the oxidative degradation cases except for the addition of 'PACT coal ash' which is seen to result in a significant increase in HEI formation. However the GC–MS measurements appear to detect high levels of HEI also for the 'Olive ash' and 'Coal ash #1'. These are not supported by the quantification of HEI using NMR.

A possible explanation for the difference observed in Fig. 7a) could be explained by a high correlation between the quantities of HEINO measured from NMR and quantities of HEI being detected with GC–MS. Specifically, higher levels of HEINO are measured for the 'Olive ash', 'Coal ash #1' and 'PACT coal ash' cases which would explain the differences seen in Fig. 7a) if HEINO in the liquid samples is being

measured by the GC–MS as HEI. The differences in measurements between these methods was found to be proportional to the amounts of HEINO measured by NMR.

The comparison of GC–MS and NMR quantities for HEF in Fig. 7 b) show a good correlation between the two measurement techniques. From this it is confirmed that slightly higher quantities of HEF are formed in the presence of 'PACT coal ash' and slightly lower quantities of HEF are observed in the presence of 'PACT wood ash', when compared to the other cases, i.e. HEF: PACT coal ash > PACT wood ash.

The oxidatively degraded MEA samples generated in the laboratory were analysed for metal impurities to measure the metals present in solution that could impact the degradation process. Results of the ICP-OES analysis, presented in Table 4, find quantities of K, Na and Mg in solution to correlate well with the quantities measured in ash composition data provided. Very low amounts of potassium are seen in the case of both coal ashes and for the MEA alone degradation, whereas significant quantities are seen in both biomass cases. It follows that more potassium is seen in the olive ash case as there is larger amounts of potassium in this ash compared to PACT wood ash, thus suggesting a similar amount of potassium is in a water-soluble state for both biomass ashes.

High quantities of Na were measured in both coal ash cases compared to MEA alone, KCl and olive. However the highest quantities
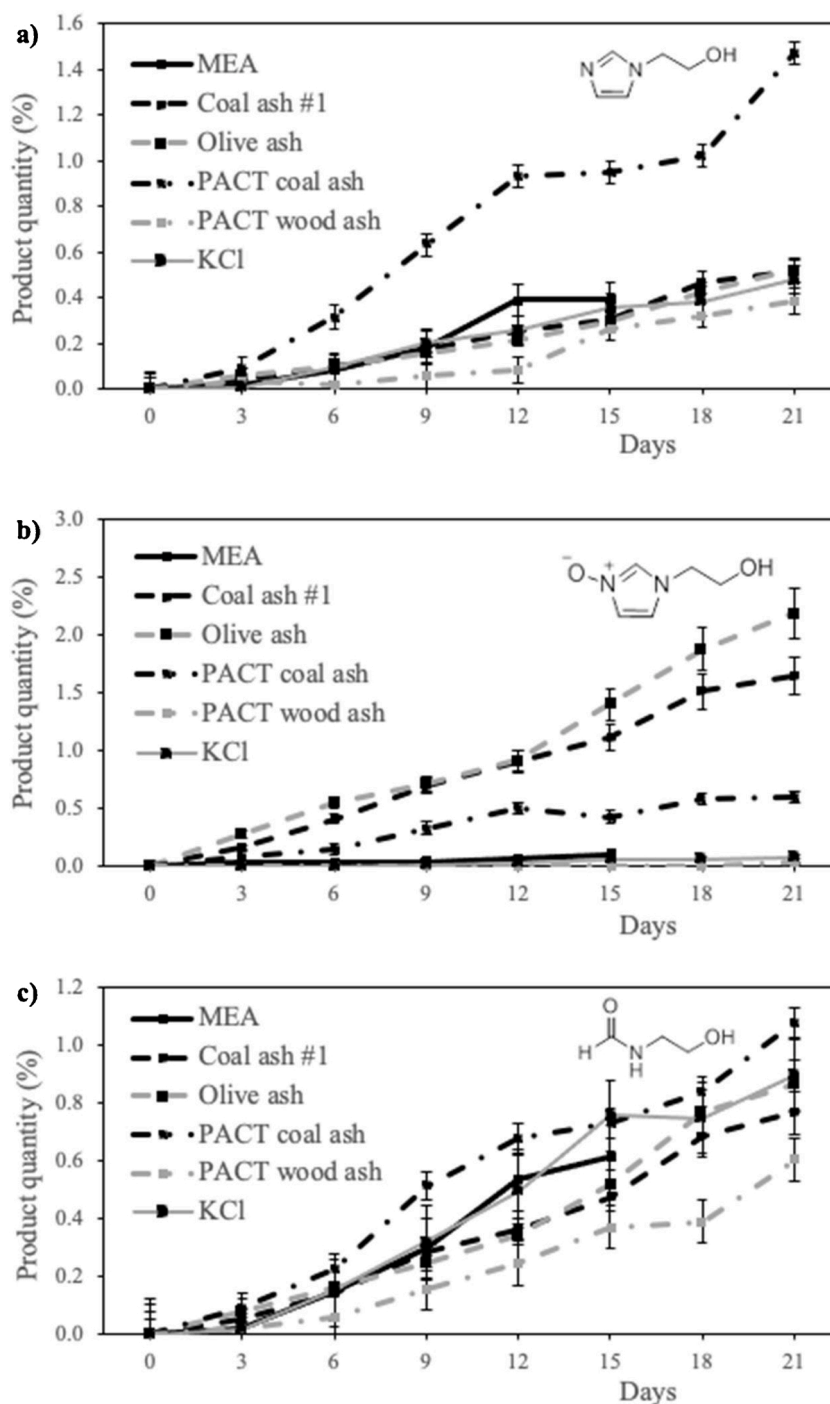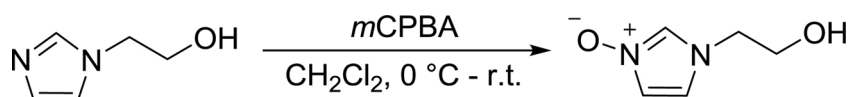
Fig. 6. Formation of a) HEI b) HEINO and c) HEF during the sparging of 30 wt% MEA with compressed air at 40 °C.

Scheme 1. Synthesis of N-(2-hydroxyethyl)imidazole-*N*-oxide (HEINO).

of Na are measured in the wood ash case. Ca, Cu, Cr, Mn and Pb are seen to be significantly higher for the white wood case. Mg is highest for both coal cases.

3.3. Degradation in a pilot-scale CO₂ capture plant

The samples of rich solvent collected from the PACT facilities at the end of each 3 day (30 h) trial were analysed for the formation of degradation products. Fig. 8 illustrates the comparative quantification of the key oxidative degradation products using ^{1}H NMR spectroscopy,
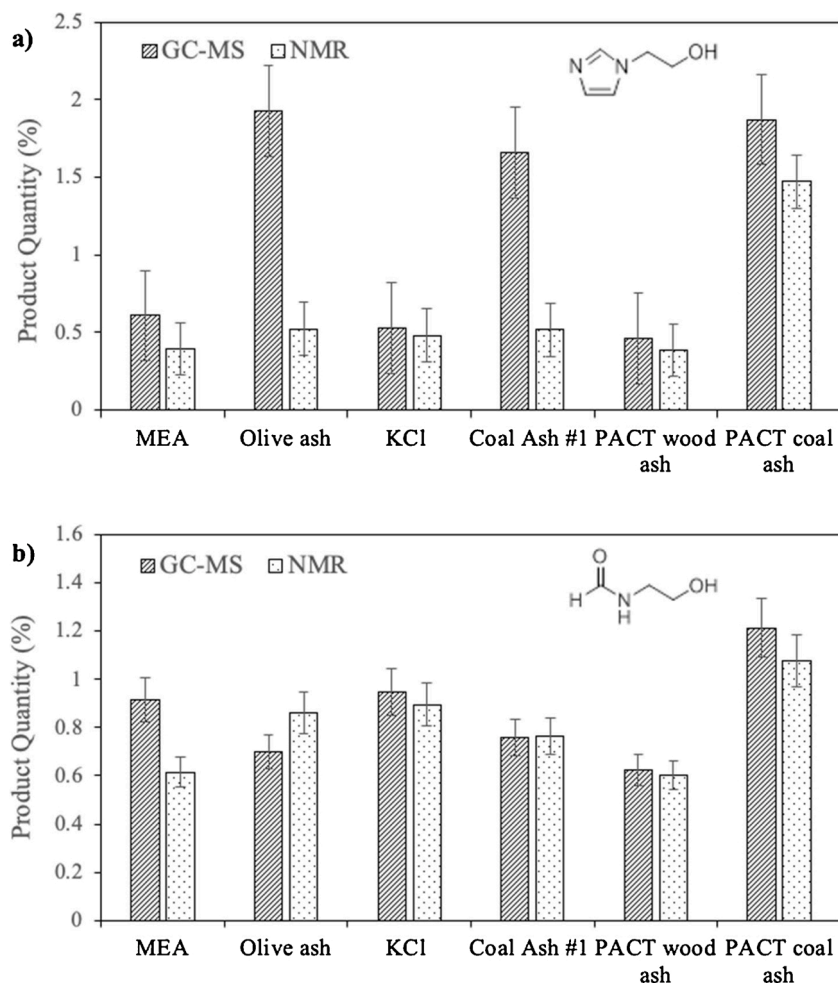

Fig. 7. Comparison of measurement techniques analysing the formation of a) HEI and b) HEF in the oxidative degradation of MEA through sparging with compressed air at 40 °C.

Table 4
Elemental accumulation analysis by ICP-OES of MEA solvents from laboratory oxidative degradations (reported to 3 significant figures).

	MEA alone (mg/L)	Olive ash (mg/L)	KCl (mg/L)	Coal ash #1 (mg/L)	PACT wood ash (mg/L)	PACT coal ash (mg/L)
Al	10.1	10.4	10.4	10.3	10.1	10.3
Mg	<LOD*	<LOD*	<LOD*	2.12	0.92	4.97
Ca	<LOQ*	28.7	<LOQ	2.07	45.8	9.18
Mn	1.19	22.4	1.37	15.7	25.1	10.3
Cu	<LOQ*	0.07	<LOQ*	0.01	0.19	0.06
Cr	<LOD*	0.41	<LOQ*	0.04	1.07	0.17
K	0.90	739	1090	3.02	512	10.2
Na	27.1	19.6	22.6	47.6	110	62.0
Fe	0.21	3.13	0.14	4.25	9.34	20.0
Si	7.16	16.5	9.39	2.28	2.27	1.40

* <LOD, below limit of detection, and < LOQ, below limit of quantification.

Fig. 8. Degradation product formation measured by NMR in 30 wt% MEA from the PACT facilities after 3-day biomass and coal combustion campaigns.

and validated with GC–MS. Much larger quantities of HEINO are measured in the solvent from the coal combustion case, whereas HEF is observed to be similar for both cases.

Interestingly, NMR analysis of the pilot scale MEA samples found no detectable HEI to be present for either case, only HEINO. GC–MS analysis is consistent with HEINO being detected as HEI during gas chromatography due to rapid degradation during analysis, hence the *N*-oxide characterised in this research was present in ratios matching that measured as HEI using GC–MS.
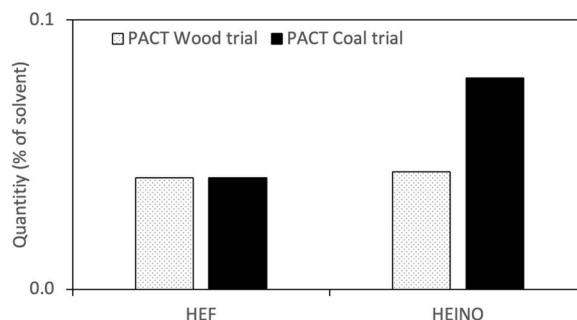
The MEA samples from the pilot-scale facility were analysed for elemental impurities to enabling the tracking of ashes and volatile species that escaped the three particle removal technologies described above. Results of the ICP-OES analysis, presented in Table 5, find high quantities of K, Ca and redox active Cr and Mn in solution from the biomass trial, compared to the coal trial. MEA samples from the coal trial where found to have more Si, Mn, Fe and Na. These findings generally correlate well with the measures of elemental oxides from ash analysis of the fuels.

Table 5

Elemental accumulation analysis by ICP-OES of MEA solvents from the PACT facilities (reported to 3 significant figures).

Element	PACT Wood (mg/L)	PACT Coal (mg/L)
Al	10.4	10.6
Mg	0.20	<LOQ
Ca	1.44	1.19
Mn	2.73	4.32
Cu	0.17	0.11
Cr	2.64	0.69
K	27.0	4.42
Na	5.73	19.2
Fe	0.58	0.81
Si	6.08	7.61

4. Discussion

4.1. Thermal degradation

The findings of the thermal degradation experiments suggest that ashes, either coal or biomass, have little impact on the formation of degradation products under thermal conditions. This is supported by other literature on thermal degradation (Davis and Rochelle, 2009; Huang et al., 2014). These experiments were complete at 135 °C to accelerate the conditions seen in a reboiler, from which the main thermal degradation products (OZD, HEEDA and HEIA) are formed. Primary and secondary aminoalcohols under thermal degradative conditions, undergo ring closure on carbamate formation to give oxazolidinones, as suggested by Polderman (1955). OZD molecules are sensitive to nucleophilic reactions and therefore can often react with another amine molecule to form a dimer such as HEEDA (Lepaumier et al., 2009b). HEEDA can cyclise to form HEIA which is the major product from thermal degradation which has been found to significantly contribute to degradation at pilot-scale facilities (Thompson et al., 2017), and as it is no longer basic, will not participate in the CO_2 capture process and hence significantly reduce solvent efficiency.

4.2. Oxidative degradation

This work used NMR spectroscopy to characterise the oxidative degradation products identified previously in literature. These characterisations were compared with NMR data from literature which revealed the incorrect assignment of NMR shifts for the most abundant oxidative degradation product, HEI. Updated NMR data is provided in this work along with characterisation of the compound previously mistaken for HEI. A new degradation product was discovered, N-(2-hydroxyethyl)imidazole-N-oxide (HEINO), which is found to be present in significant quantities in some cases, and the two species are likely to be interconverted depending on the process conditions.

Results from the oxidative degradation experiments suggest that ashes from coal and olive combustion can enhance the formation of HEINO, whereas only one of the coal ashes appears to catalyse the formation of the previously identified major oxidative degradation product, HEI. The comparison of fly ashes collected from the PACT facilities shows higher rates of HEI and HEINO formation with coal ash compared to wood ash. Slower rates of HEI, HEINO and HEF formation were seen for the wood ash collected from the PACT facilities compared to all other cases.

This work has shown that the composition of an ash can have a large impact on the formation of amine degradation products. For example, the coal fly ash collected from the PACT facilities (PACT coal ash) showed a larger production of HEI than the other ashes but lower amounts of HEINO than coal ash #1 and the olive ash. This appears to suggest that the PACT coal ash may favour the formation of HEI with little subsequent oxidation to HEINO. Fig. 9 plots the total of the integrated NMR peaks at shift: 7.21 ppm for HEINO, 7.03 ppm for HEI and
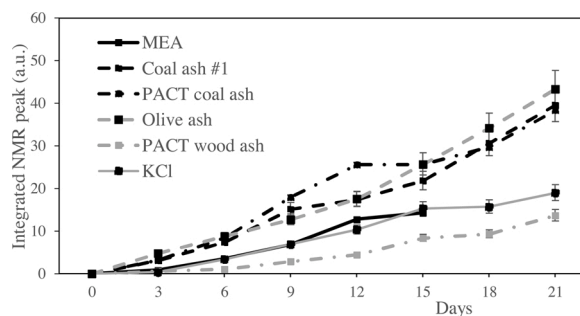

Fig. 9. The combined integration of NMR peaks of HEI, HEF and HEINO relative to DSS standard, for a cumulative plot of the major degradation products formed in each case.

8.09 ppm for HEF. This comparison suggests that olive ash produces the largest total quantities of degradation products, followed by the coal ash #1 and PACT coal ash, and that the PACT wood ash and KCl have negligible effects on the formation of imidazoles or HEF.

OZD and HEF appear less affected by the addition of ash. It has been suggested that HEA and HEF are formed through MEA reacting with acidic oxidised degradation products, such as acetic acid and formic acid respectively (Da Silva et al., 2012). The formation of HEI is less understood than the other oxidative constituents, however it has been confirmed that HEI can be formed from the mixing of MEA, formaldehyde, glyoxal and ammonia which are all known products and fragments of MEA degradation (Vevelstad et al., 2013) although levels of some of these are rather low, and alternative pathways are also likely.

The results suggest that white wood ash and KCl have negligible effects on the formation of imidazoles, however other types of biomass that could be used in BECCS plants, such as olive residues, may have different impacts on amine degradation.

Ammonia, methylamine, formaldehyde and acetaldehyde are the initial products formed from the oxidation of MEA. Carboxylic acids, such as formic, acetic, glycolic and oxalic have been previously identified and reaction pathways have been suggested (Rooney et al., 1998; Strazisar et al., 2003). Ammonia is likely formed from the oxidation and hydrolysis, or fragmentation of the MEA molecule, whereas the acids are from further oxidation aldehydes, also formed from MEA (Da Silva et al., 2012; Lepaumier et al., 2009a).

These primary degradation products are found to degrade further to form secondary degradation compounds from reaction with oxygen, MEA, aldehydes or ammonia. The major secondary oxidative degradation products are N-(2-hydroxyethyl) formamide (HEF) and N-(2-hydroxyethyl) imidazole (HEI) are more stable and arguably more likely to have an impact on the performance of carbon capture solvents than primary degradation products (Reynolds et al., 2015). The mechanisms by which these secondary products could be formed are not well understood, though mechanisms have been suggested in literature whereby HEF could be formed from the reaction of formic acid with MEA (Da Silva et al., 2012; Lepaumier et al., 2011; Strazisar et al., 2003).

HEI is the most abundantly observed degradation product from the oxidation of MEA. The finding of a previously undiscovered degradation product by this work, HEINO, which is found to be present in significant quantities may be the result of two options. Either HEI is readily oxidised during the oxidative degradation process to form HEINO as a final degradation product, and they form part of a redox cycle within the process. Alternatively HEINO is formed as an intermediary compound in the formation of HEI, with it being reduced in the final step. The variation in quantities of HEI and HEINO between the different degradation cases would suggest that there may be an equilibrium between the two redox states, and that different ashes can alter the equilibrium resulting in differing ratio quantities of each product, possibly due to the presence of different levels of redox active metals, or the history of particular

samples, and where they were removed from the process, e.g. post-absorber, post-stripper, etc.

4.3. Pilot-plant degradation

Real world post combustion capture (PCC) processes are not simple. Amines encounter fluctuating temperatures, varying flue gas composition and differences in ambient conditions which can impact on performance. The biomass and coal combustion and PCC campaigns were completed using the same equipment and fuel feed rates however the campaigns were conducted at different times, and the SOx removal equipment was only operational for 2 days of the coal combustion campaign. Similar quantities of the main thermal degradation product, HEIA, and a major oxidative degradation product, HEF, are measured for both pilot-scale combustion cases suggesting that the temperatures that both solvents were exposed to were similar and that temperature was not a factor in the differences in degradation.

^{1}H NMR analysis found HEINO to be the most abundant secondary degradation product formed in these pilot-scale samples. This is an interesting result as it suggests that HEINO may be the dominant imidazole species occurring under true carbon capture conditions.

Solvent samples obtained from the PACT facilities matched the findings of the laboratory-scale oxidative degradation experiments of this study. The pilot plant was not run for a long period thus not enabling the in-depth comparison of the prolonged degradation between coal and biomass flue gases. However these results show the early formation of oxidative degradation products (HEF and HEINO). The analysis observed lower quantities of HEINO in the biomass test campaign compared to coal.

The elemental analysis of MEA samples from the pilot-scale facility showed that high quantities of K from biomass combustion remained in the flue gas after three forms of flue gas treatment, likely due to its volatile state as identified in previous work at the PACT facilities (Finney et al., 2018). Higher quantities of Ca and Cr were measured in the MEA sample from the biomass trial than the coal trial (Table 5), whereas the coal trial samples contained more Si, Mn, Fe and Na. These findings generally correlate well with the measures of elemental oxides from ash analysis of the fuels suggesting that some fly-ashes were deposited in the amine capture solvent and may explain the higher quantities of degradation products measured for the coal trial due to presence of more catalytically active metals for oxidation.

5. Conclusion

This work has demonstrated the potential for NMR spectroscopy to be applied to the carboxylation and degradation of MEA. ^{1}H and ^{13}C NMR analysis have been successfully used to monitor the formation of previously identified major degradation products (OZD, HEEDA, HEIA, HEI and HEF). Full NMR data for MEA, carbamate and the degradation products are provided. Revised NMR chemical shift data is provided for existing degradation products and a new degradation product has been identified, *N*-(2-hydroxyethyl)imidazole-*N*-oxide (HEINO), which in some cases is the most abundant degradation product including the MEA samples obtained from a pilot-scale combustion and carbon capture facility.

This research has examined the impact that fly ashes from biomass combustion will have on amine degradation compared to coal fly ashes. The results of laboratory testing in this study has found biomass ashes from white wood combustion to reduce the formation of the major oxidative degradation products by more than half. Samples obtained from 3-day pilot-scale air-biomass and air-coal trials at the PACT facilities support these findings. Carbon capture processes are complex and more research is required before conclusions can be drawn on the degradation of amines in a full scale BECCS plant. The complexity of degradation will increase with continued use of amine blends and other amine structures, however these initial findings suggest the carbon capture applied to flue gases from white wood biomass combustion may observe less amine degradation, and thus reduced regeneration costs, than coal or olive biomass plant combustion.

Author statement

Diarmaid S. Clery is a PhD student who carried out the majority of the practical work.

Patrick E. Mason worked with DSC including substantial help with analysis.

János Szuhánszki and Muhammad Akram are responsible for the operational aspects of the pilot scale PACT facility.

Jenny M. Jones is a co-supervisor for DSC and advised on areas such as biofuels selection and analysis.

Mohamed Pourkashanian has overall reposnsibility for the PACT facility.

Christopher M. Rayner supervised the majority of the research work in this paper and has been responsible for writing it alongside DSC.

Douglas C. Barnes provided ongoing industrial and chemistry input to the research, and helped supervise DSC when he was on placement at C-Capture.

Declaration of Competing Interest

The authors declare the following financial interests/personal relationships which may be considered as potential competing interests:

Dr Douglas Barnes is an employee of, and shareholder in C-Capture Ltd. who specialize in the development and commercialisation of amine-free solvents for solvent based post-combustion CCS. Prof. Rayner is Founder and a Director of C-Capture and is also a shareholder.

Appendix A. Supplementary data

Supplementary material related to this article can be found, in the online version, at doi:https://doi.org/10.1016/j.ijggc.2021.103305.

References

Akram, M., Ali, U., Best, T., Blakey, S., Finney, K.N., Pourkashanian, M., 2016. Performance evaluation of PACT Pilot-plant for CO_2 capture from gas turbines with Exhaust Gas recycle. Int. J. Greenh. Gas Control 47, 137–150.

Anderson, K., Peters, G., 2016. The trouble with negative emissions. Science 354 (6309), 182–183.

Bui, M., Adjiman, C.S., Bardow, A., Anthony, E.J., Boston, A., Brown, S., Fennell, P.S., Fuss, S., Galindo, A., Hackett, L.A., Hallett, J.P., Herzog, H.J., Jackson, G., Kemper, J., Krevor, S., Maitland, G.C., Matuszewski, M., Metcalfe, I.S., Petit, C., Puxty, G., Reimer, J., Reiner, D.M., Rubin, E.S., Scott, S.A., Shah, N., Smit, B., Trusler, J.P.M., Webley, P., Wilcox, J., Mac Dowell, N., 2018. Carbon capture and storage (CCS): the way forward. Energy Environ. Sci. 1062–1176.

Chandan, P., Richburg, L., Bhatnagar, S., Remias, J.E., Liu, K., 2014. Impact of fly ash on monoethanolamine degradation during CO_2 capture. Int. J. Greenh. Gas Control 25, 102–108.

Ciftja, A.F., Hartono, A., Grimstvedt, A., Svendsen, H.F., 2012. NMR study on the oxidative degradation of MEA in presence of Fe^{2+}. Energy Procedia 23, 111–118.

Clery, D.S., 2019. The Fate of Potassium and Ash From Biomass Combustion and Their Impact on the Degradation of Monoethanolamine (MEA) for Carbon Capture. PhD Thesis. University of Leeds.

Clery, D.S., Mason, P.E., Rayner, C.M., Jones, J.M., 2018. The effects of an additive on the release of potassium in biomass combustion. Fuel 214, 647–655.

Da Silva, E.F., Lepaumier, H., Grimstvedt, A., Vevelstad, S.J., Einbu, A., Vernstad, K., Svendsen, H.F., Zahlsen, K., 2012. Understanding 2-ethanolamine degradation in postcombustion CO_2 capture. Ind. Eng. Chem. Res. 51, 13329–13338.

Davis, J., Rochelle, G., 2009. Thermal degradation of monoethanolamine at stripper conditions. Energy Procedia 1, 327–333.

Dumée, L., Scholes, C., Stevens, G., Kentish, S., 2012. Purification of aqueous amine solvents used in post combustion CO_2 capture: a review. Int. J. Greenh. Gas Control 10, 443–455.

Finney, K., Szuhánszki, J., Darvell, L., Dooley, B., Milkowski, K., Jones, J.M., Pourkashanian, M., 2018. Entrained metal aerosol emissions from air-fired biomass and coal combustion for carbon capture applications. Materials (Basel). 11, 1819–1834.

Fuentes, J.A., Clarke, M.L., 2008. Deoxygenation of pyridine N-oxides by palladium-catalysed transfer oxidation of trialkylamines. Synlett. 17, 2579–2582.

Goff, G.S., 2005. Oxidative Degradation of Aqueous Monoethanolamine in CO_2 Capture Processes: Iron and Copper Catalysis, Inhibition, and O_2 Mass Transfer. PhD Thesis. University of Texas at Austin.

Goff, G.S., Rochelle, G.T., 2006. Oxidation inhibitors for copper and iron catalyzed degradation of monoethanolamine in CO_2 capture processes. Ind. Eng. Chem. Res. 45, 2513–2521.

He, W., Xie, L., Xu, Y., Xiang, J., Zhang, L., 2012. Electrophilicity of α-oxo gold carbene intermediates: Halogen abstractions from halogenated solvents leading to the formation of chloro/bromomethyl ketones. Org. Biomol. Chem. 10 (16), 3168–3171.

Huang, Q., Thompson, J., Bhatnagar, S., Chandan, P., Remias, J.E., Selegue, J.P., Liu, K., 2014. Impact of flue gas contaminants on monoethanolamine thermal degradation. Ind. Eng. Chem. Res. 53, 553–563.

IPCC, 2018. Global Warming of 1.5 °C - Summary for Policymakers.

Jones, J.M., Darvell, L.I., Bridgeman, T.G., Pourkashanian, M., Williams, A., 2007. An investigation of the thermal and catalytic behaviour of potassium in biomass combustion. Proc. Combust. Inst. 31, 1955–1963.

Knudsen, J.N., Jensen, P.A., Dam-Johansen, K., 2004. Transformation and release to the gas phase of Cl, K, and S during combustion of annual biomass. Energy Fuels 18, 1385–1399.

Léonard, G., Toye, D., Heyen, G., 2015. Relevance of accelerated conditions for the study of monoethanolamine degradation in post-combustion CO_2 capture. Can. J. Chem. Eng. 93, 348–355.

Lepaumier, H., Picq, D., Carrette, P.L., 2009a. New amines for CO_2 capture. II. Oxidative degradation mechanisms. Ind. Eng. Chem. Res. 48, 9068–9075.

Lepaumier, H., Picq, D., Carrette, P.L., 2009b. New amines for CO_2 capture. I. Mechanisms of amine degradation in the presence of CO_2. Ind. Eng. Chem. Res. 48, 9061–9067.

Lepaumier, H., Da Silva, E.F., Einbu, A., Grimstvedt, A., Knudsen, J.N., Zahlsen, K., Svendsen, H.F., 2011. Comparison of MEA degradation in pilot-scale with lab-scale experiments. Energy Procedia 4, 1652–1655.

Mason, P.E., Darvell, L.I., Jones, J.M., Williams, A., 2016. Observations on the release of gas-phase potassium during the combustion of single particles of biomass. Fuel 182, 110–117.

Murray, J., 2016. Preparation of 1-methylimidazole-N-oxide (NMI-O). Organic Synth. 93, 331–340.

Niu, B., Nie, Q., Huang, B., Cai, M., 2019. Heterogeneous gold(I)-catalyzed oxidative ring expansion of 2-alkynyl-1,2-dihydropyridines or -quinolines towards functionalized azepines or benzazepines. Adv. Synth. Catal. 361, 4065–4074.

Perinu, C., Arstad, B., Jens, K.J., 2014. NMR spectroscopy applied to amine-CO_2-H_2O systems relevant for post-combustion CO_2 capture: a review. Int. J. Greenh. Gas Control 20, 230–243.

Polderman, L.D., Dillon, C.P., Steele, A.B., 1955. Why monoethanolamine solution breaks down in gas treating service. Oil Gas J. 54, 180–183.

Reynolds, A.J., Verheyen, T.V., Adeloju, S.B., Chaffee, A.L., Meuleman, E., 2015. Evaluation of methods for monitoring MEA degradation during pilot scale post-combustion capture of CO_2. Int. J. Greenh. Gas Control 39, 407–419.

Rooney, P.C., Dupart, M.S., Bacon, T.R., 1998. Oxygen's role in alkanolamine degradation. Hydrocarb. Process. 109–113.

Sexton, A., Rochelle, G., 2006. Oxidation products of amines in CO_2 capture. 8th Int. Conf. Greenh. Gas Control Technol 1–6.

Sexton, A.J., Rochelle, G.T., 2009. Catalysts and inhibitors for MEA oxidation. Energy Procedia 1, 1179–1185.

Strazisar, B.R., Anderson, R.R., White, C.M., 2003. Degradation pathways for monoethanolamine in a CO_2 capture facility. Energy Fuels 17, 1034–1039.

Szuhánszki, J., 2014. Advanced Oxy-Fuel Combustion for Carbon Capture and Sequestration. PhD Thesis. University of Leeds.

Thompson, J.G., Combs, M., Abad, K., Bhatnagar, S., Pelgen, J., Beaudry, M., Rochelle, G., Hume, S., Link, D., Figueroa, J., Nikolic, H., 2017. Pilot testing of a heat integrated 0.7 MWe CO_2 capture system with two-stage air-stripping: Emission. Int. J. Greenh. Gas Control 64, 267–275.

Vevelstad, S.J., Grimstvedt, A., Elnan, J., da Silva, E.F., Svendsen, H.F., 2013. Oxidative degradation of 2-ethanolamine: the effect of oxygen concentration and temperature on product formation. Int. J. Greenh. Gas Control 18, 88–100.

Wheatley, J.E., 2017. Fundamental Chemistry of Carbon Dioxide Capture. PhD Thesis. University of Leeds.

Wheatley, J.E., Bala, S., Barnes, D.C., Schoolderman, C., Jakab, G., Raynel, G., Rayner, C.M., 2019. CO_2 Capture using phenoxide salts; alternatives to amine-based capture agents, and comparative speciation studies as components in solvent blends. Int. J. Greenh. Gas Control 88, 353–360.